Forest Ecology and Management 258 (2009) 306–313

Contents lists available at ScienceDirect

Forest Ecology and Management

journal homepage: www.elsevier.com/locate/foreco

Growth–climate responses of high-elevation conifers in the central Hengduan Mountains, southwestern China

Ze-Xin Fan [a,b], Achim Bräuning [b,*], Kun-Fang Cao [a], Shi-Dan Zhu [a]

[a] Key Laboratory of Tropical Forest Ecology, Xishuangbanna Tropical Botanical Garden, Chinese Academy of Sciences, 88 Xuefu Road, Kunming 650223, China
[b] Institute of Geography, University of Erlangen-Nürnberg, Kochstrasse 4/4, D-91054 Erlangen, Germany

ARTICLE INFO

Article history:
Received 29 January 2009
Received in revised form 20 April 2009
Accepted 20 April 2009

Keywords:
Hengduan Mountains
Tree-rings
Dendroclimatology
Climate change

ABSTRACT

Improved understanding of tree-growth responses to climate is needed to model and predict forest ecosystem responses to current and future climatic variability. We applied dendroclimatological techniques to assess the effects of inter-annual climate variations on radial growth of high-elevation conifers in the central Hengduan Mountains, southwestern China. Eight tree-ring width chronologies of the major tree genera *Abies* and *Picea* that are aligned along an elevation gradient from 3200 to 4200 m a.s.l. were developed. Correlation and principal component analyses for the eight chronologies identified three groups of sites, representing different patterns of growth–climate relationships. Correlation and redundancy analyses with regional climate data revealed that radial growth of fir growing at high-elevation sites is enhanced by normal or warm summer temperatures (June and July) during the current growing season. In addition, radial growth of trees growing from high to middle elevations is sensitive to low temperatures during winter season. At low-elevation sites, trees display low sensitivity to temperature variation. However spring moisture availability becomes crucial for radial growth regardless of tree species. High- to middle-elevation conifers in the central Hengduan Mountains may benefit from the current climate warming, especially from rising winter temperatures.

1. Introduction

Tree-ring growth responses to climate change provide crucial information to assess future forest productivity, vegetation dynamics and tree-species distributions (e.g. Peterson and Peterson, 2001; Saxe et al., 2001; Frenzel et al., 2003; Thuiller et al., 2005; Tardif et al., 2006). Furthermore, climate–growth relationships are the basis for tree-ring based climate reconstructions (Briffa et al., 1998; Tessier et al., 1997). The physiological mechanisms by which climatic parameters are translated into radial growth variations are complex, because radial growth in any given year integrates the effects of climate conditions during and prior to growth, local site conditions and physiological characteristics of tree species (Fritts, 1976). In mountain regions, radial growth of trees at high elevations generally reflects temperature variations, whereas growth rates of trees at lower elevations generally mirror precipitation changes (Schweingruber, 1996). However, because of the co-variation of various climatic parameters and complex plant physiological reactions and processes, attempts to define growth responses in terms of a single controlling factor often fail (Fritts, 1976). For example, even at cold sites, water availability during the short vegetation period becomes the dominating factor for tree growth, when temperature is high enough (e.g. Anfodillo et al., 1998; Carrer et al., 1998).

With an average elevation of more than 4000 m a.s.l., the Tibetan Plateau is one of the most sensitive regions to climate change (Zheng, 1996). In recent years, considerable efforts have been made to reconstruct past climate change on the Tibetan Plateau. In the course of these studies, growth–climate relationships in different regions and across environmental gradients were evaluated (e.g. Bräuning, 1994, 2001; Zhang et al., 2003; Shao et al., 2005; Liang et al., 2006, 2008). However, the Tibetan Plateau covers an area of more than 2 million km^2 and regional climate conditions are far from uniform but vary considerably according to topographic conditions and exposure to moisture bringing winds. In the semi-arid cold regions of the northeastern Tibetan Plateau, radial growth of *Sabina przewalskii* and *Picea crassifolia* are mainly influenced by late-spring to early summer (April–June) precipitation. This reaction pattern has been found in the Qilian Mountains (Gou et al., 2005; Tian et al., 2007), in the Dulan area (Zhang et al., 2003; Sheppard et al., 2004; Shao et al., 2005; J. Li et al., 2008) and in the Anyemaqen Mountains (Gou et al., 2007a). However, the effects of spring or summer precipitation on radial growth of these species vanish at high-elevation sites (Liu et al., 2006; Peng et al., 2008). The same holds true for north- and east-facing slopes (Liang et al., 2006) where higher amounts of moisture for tree growth are

* Corresponding author. Tel.: +49 9131 8529372; fax: +49 9131 8522013.
E-mail address: abraeuning@geographie.uni-erlangen.de (A. Bräuning).

0378-1127/$ – see front matter © 2009 Elsevier B.V. All rights reserved.
doi:10.1016/j.foreco.2009.04.017

available than on south-facing slopes. At high elevations, conifers are more sensitive to temperature variations during winter as well as during the summer season (Shao and Fan, 1999; Bräuning, 2001; Liang et al., 2008).

The north–south oriented Hengduan Mountains form the southeastern rim of the Tibetan Plateau. The region is extremely rich in conifer species and is an important refuge area where conifers survived in the harsh conditions during the cold climate stages during the Pleistocene, when Tibet was free of forest (Frenzel et al., 2003). Presently, the region is covered by widespread forests dominated by various coniferous species and thus has a great potential for dendroclimatological studies (Wu et al., 1988; Bräuning, 1994; Fan et al., 2008). To improve our understanding of tree-rings as proxies for climate reconstructions and to estimate the ecological responses of subalpine trees to climate change, profound knowledge about the influence of climatic variables on tree growth is needed. In this study, we contribute new data about climate–growth relationships of major forest types that are characteristic for different environmental conditions within this ecological complex area.

2. Materials and methods

2.1. Study area and climate

The study area is located in the central Hengduan Mountains, southwestern China (Fig. 1). The mountain ranges run roughly north to south and separate major Asian rivers, namely Jinsha Jiang (upper Yangtze), Lancang Jiang (upper Mekong) and Nu Jiang (upper Salween). They converge within a corridor stretching only 90 km from east to west in the central portion of the Hengduan Mountains. The resulting landscape patterns include extreme topographic gradients between deeply incised parallel gorges in ca. 1500 m a.s.l. and glaciated peaks in over 6700 m a.s.l. within a distance of 20 km or even less. The pronounced altitudinal climatic gradients lead to a differentiation of mountain forests into altitudinal belts. The dry valleys are usually covered by scrublands and are presently free of forest. Above this belt which is also strongly influenced by human activity, mixed forests of broad-leaved and sclerophyllous oak species occur. Cold-temperate coniferous forests cover the subalpine vegetation zone from 3000 m a.s.l. up to the upper treeline. They are dominated by spruce (*Picea brachytyla*, *P. likiangensis*), fir (*Abies georgei*, *A. forrestii*) and larch species (*Larix potaninii*). The soil types are brown and dark brown coniferous forest soils. The upper timberline in the area is formed by fir and is situated at ca. 4000 m a.s.l., whereas isolated trees reach even higher than 4200 m a.s.l. Due to the high absolute elevation of the valley floors (around 2000 m a.s.l.), we will refer to high-, middle- and low-elevation sites in the context of this study as locations situated above 3600 m, between 3300 and 3600 m and below 3300 m, respectively (Table 1).

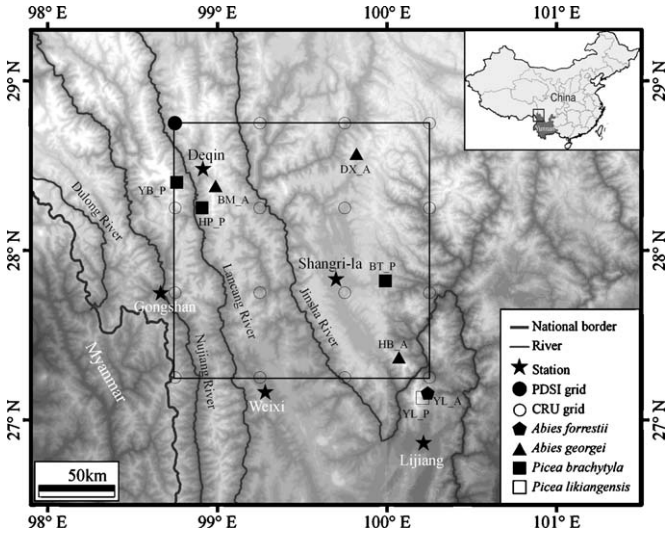

Fig. 1. Locations of tree-ring sites and meteorological stations in the central Hengduan Mountains, southwestern China. Square highlights the area covered by 16 gridded climate data points of CRUts2.1 (0.5 × 0.5; Mitchell and Jones, 2005).

The climate of this region is strongly influenced by the south Asian summer monsoon during June–September. As recorded from three meteorological stations (Fig. 2), mean annual temperatures range from 5.2 to 12.6 °C, the annual sum of precipitation ranges from 644 to 970 mm, 60–80% of which fall during the summer monsoon season from June–September. During the winter season, continental air masses (East Asian winter monsoon) of the central Asian high pressure cell dominate and lead to very cold and dry conditions with occasional surges of dry continental polar air from northwesterly directions (Böhner, 2006). Temperature lapse rate during summer is ~0.57 °C per 100 m elevation increase (Zhang, 1998). Precipitation decreases from south to north along the passageways of the monsoonal air masses (Fig. 2). Precipitation increases with increasing elevation. For example, at the east slope of the Baima Snow Mountain, the annual sum of precipitation increases by 10–50 mm per 100 m elevation increase (The Editing Committee of "The Baima National Nature Reserve", 2003).

2.2. Tree-ring sampling and chronology development

Our sampling sites are situated in the mountain ranges between the Lancang and Jinsha River (Fig. 1). The sites are located in six Nature Reserves: Meili Snow Mountain (YB_P), Baima Snow Mountain (BM_A and HP_P), Daxueshan (DX_A), Bitahai National Park (BT_P), Haba Snow Mountain (HB_A) and Yulong Snow Mountain (YL_A, YL_P; note that _A stands for fir sites and _P for spruce sites). Increment cores from living fir (*A. georgei* and *A. forrestii*) and spruce (*P. brachytyla* and *P. likiangensis*) trees were

Table 1
Tree-ring site locations and chronology characteristics.

Site	Elevation level	Species	Aspect	Slope (°)	Latitude (N)	Longitude (E)	Elev. (m)	MSL	AGR (mm)
DX_A	*High*	*A. georgei*	N	35	28.57	99.82	4200	150	0.76
BM_A	*High*	*A. georgei*	W	28	28.38	98.99	4100	237	0.57
HB_A	*Middle*	*A. georgei*	SE	22	27.37	100.07	3400	146	1.06
YL_A	*Low*	*A. forrestii*	E	<10	27.16	100.24	3250	149	1.88
BT_P	*Middle*	*P. brachytyla*	NW	16	27.82	99.99	3580	234	0.81
HP_P	*Middle*	*P. brachytyla*	NW	24	28.25	98.91	3500	186	1.40
YB_P	*Middle*	*P. brachytyla*	E	12	28.40	98.76	3380	218	1.25
YL_P	*Low*	*P. likiangensis*	E	<10	27.14	100.22	3200	277	1.07

DX_A, Daxueshan; BM_A, Baima Snow Mountain; HB_A, Haba Snow Mountain; YL_A, YL_P, Yulong Snow Mountain; BT_P, Bitahai Nature Reserve; HP_P, Hongpo at Baima Snow Mountain; YB_P, Yubeng at Meili Snow Mountain; Elev., elevation; MSL, mean segment length; AGR, average growth rate.

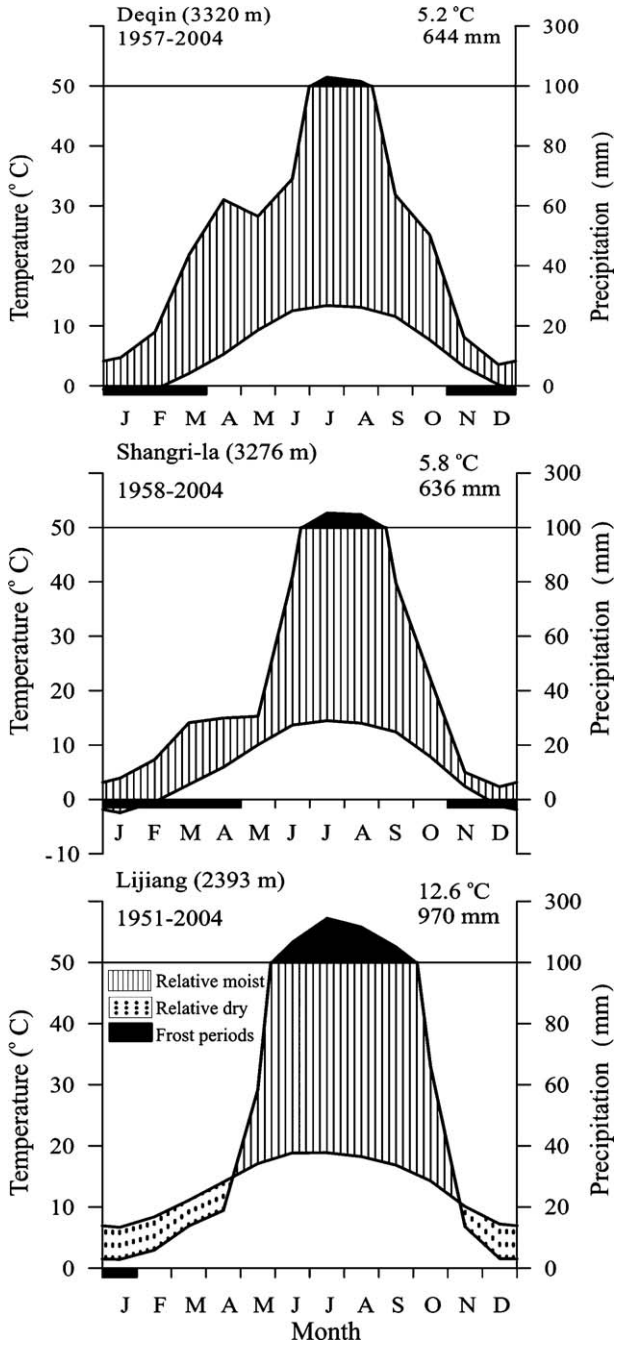

Fig. 2. Climate diagrams for the three meteorological stations in the central Hengduan Mountains, southwestern China.

collected from eight sites (Fig. 1). In total, 202 trees (302 cores) were sampled at breast height with an increment borer, with a minimum of 14 trees at each site (Tables 1 and 2). The cores were mounted on sample holders and the wood surfaces were prepared with sharp razor blades. Ring widths were measured with a LINTAB II measuring system with a resolution of 0.01 mm, and all cores were cross-dated by visual inspection (Stokes and Smiley, 1968) and by statistical tests (sign-test and *t*-test) using the software package TSAP-Win (Rinn, 2003).

Mean ring-width index chronologies were developed using the program ARSTAN (Cook, 1985). Prior to standardization, a data-adaptive power transformation was applied to reduce the heteroscedastic behavior of tree-ring series (Cook and Peters, 1997). The tree-ring series were detrended by adjusting a negative exponential or a linear regression function to the raw data. Then the resulting sequences were detrended with a cubic smoothing spline with a 50% frequency–response cut-off equal to 2/3 of the series length. Tree-ring indices were obtained by calculating differences between the transformed ring-width measurements and the fitted splines. This detrending method maximizes the common signal among individual tree-ring series, while low-frequency trends due to tree aging and stand dynamics are removed. Autoregressive modeling was used to remove persistence from each series, producing pre-whitened "residual" indices (Cook, 1985). All detrended series were averaged to chronologies by computing the biweight robust mean in order to reduce the influence of outliers (Cook and Kairiukstis, 1990). Variance stabilization (Osborn et al., 1997) was applied to adjust for changes in variance associated with declining sample size (number of trees) over time.

Several descriptive statistics were calculated for the standardized chronologies. The standard deviation (SD) estimates the variability of measurements for the whole series; the mean sensitivity (MS) is an indicator of the relative changes in ring-width variance between consecutive years; the first-order autocorrelation (AC1) assesses relationships with previous growth (Fritts, 1976). Common signal strength was evaluated by mean inter-series correlation (R_{bt}) and by the percent variance explained by the first principal component (PC#1). The expressed population signal (EPS) and signal-to-noise ratio (SNR) are functions of R_{bt} and sample size, and evaluate the signal strength of the site chronologies. A level of 0.85 for EPS is considered to indicate a satisfactory quality of a chronology (Wigley et al., 1984). To assess the similarity among the eight individual residual chronologies, correlation and principal component analyses (PCA) were applied over the common period 1850–1999.

2.3. Evaluation of climate–growth relationships

Meteorological stations in this region are sparse and generally located in the valley floors. In order to emphasize the spatial

Table 2
Descriptive statistics of the eight ring-width chronologies.

Site	Cores	Trees	Period	SD[a]	MS[a]	AC1[a]	R_{bt}[b]	EPS[b]	PC1[b]	SNR[b]
DX_A	26	17	1718–2004	0.25	0.14	0.73	0.54	0.93	45	14.1
BM_A	49	24	1651–1999	0.26	0.14	0.79	0.47	0.94	30	16.4
HB_A	18	14	1760–2007	0.26	0.16	0.70	0.37	0.74	29	2.7
YL_A	32	19	1723–2005	0.32	0.24	0.58	0.53	0.93	39	13.3
BT_P	50	40	1623–2007	0.22	0.14	0.65	0.48	0.96	37	23.1
HP_P	80	51	1688–2007	0.28	0.18	0.70	0.59	0.97	36	36.1
YB_P	15	15	1696–2003	0.24	0.15	0.71	0.39	0.80	29	4.1
YL_P	32	22	1641–2006	0.28	0.18	0.72	0.50	0.92	36	12.1

SD, standard deviation; MS, mean sensitivity; AC1, first-order autocorrelation; R_{bt}, mean inter-series correlation; EPS, expressed population signal; PC1, percent variance explained by the first principal component (PC1); SNR, signal-to-noise ratio.
[a] Calculated for the standardized chronologies prior to autoregressive modeling.
[b] Calculated for pre-whitened chronologies over the common period 1900–1999.

representation, monthly mean temperatures (TEM) and precipitation (PRE), as well as monthly mean minimum (T_{min}) and maximum temperatures (T_{max}), from a high resolution (0.5° × 0.5°) gridded dataset were used (CRUts2.1; Mitchell and Jones, 2005). Mean values were calculated from 16 grid-boxes which cover the region 27.25–28.75°N and 98.75–100.25°E over the 1951–2002 period. Monthly Palmer drought severity index (PDSI) series were used to test the influence of soil moisture on tree growth. The grid point closest to our sampling sites (28.75°N and 98.75°E) was extracted from a global PDSI dataset on a 2.5° × 2.5° grids for the period 1951–2002 (Dai et al., 2004).

Relationships between site chronologies and climate parameters were analyzed using both redundancy analysis (RDA; Trouet et al., 2001; Tardif et al., 2006) and correlation functions (Blasing et al., 1984). RDA is a multivariate "direct" gradient analysis and its ordination axes are constrained to represent linear combinations of supplied environmental variables (Legendre and Legendre, 1998). RDA may be understood as a two-step process: (1) the tree-ring chronologies are regressed on the climate variables and the fitted values are computed and (2) a PCA is then carried out on the matrix of fitted values to obtain the eigen values and eigen vectors (Legendre and Legendre, 1998; Girardin et al., 2006). The climate variables were selected using a forward selection on the basis of the goodness of fit and tested for significance using a Monte Carlo permutation test based on 999 random permutations. This procedure was repeated until a variable was tested non-significant at the 5% level.

Climate data set included monthly data over a 16-month window, from July of the year prior to tree growth until the current year October. The RDA was carried out for pooled eight chronologies and 64 climate variables over the common interval 1951–2002, using the program CANOCO (Version 4.5; ter Braak and Smilauer, 2002). Pearson's correlation coefficients were calculated over the same period for detailed growth response assessment. In addition, various seasonal means of climate variables were correlated with site chronologies and scores of the significant PCs resulting from principal component analyses.

3. Results and discussion

3.1. Internal chronology statistics

Tables 1 and 2 list the locations and descriptive statistics respectively, of the eight ring-width chronologies. The chronologies cover the last 200–350 years, with mean tree ages ranging from 150 years (HB_A) to 280 years (YL_P). Low mean growth rates are associated with increasing elevation and stand age. The chronologies generally display a low year-to-year variability (mean sensitivity, MS), which is typical for conifers growing in humid environments. However, chronologies from lower elevation sites (e.g. YL_A and YL_P) display a higher standard deviation (SD) and MS (Table 2 and Fig. 2). Trees from dry forest habitats often show higher inter-annual growth variability than trees from temperature-limited sites (Fritts, 1976; Bräuning, 2001; Liang et al., 2006). The trees from lower elevations probably suffer more from occasional moisture stress than those growing at higher elevation sites. The high first-order autocorrelations (AC1) reflect a high persistence of the ring-width chronologies, indicating a significant impact of previous year's climate on current year's ring width, probably caused by carry-over effects of carbohydrates used for early wood formation (Fritts, 1976).

Mean inter-series correlations (R_{bt}) range from 0.37 to 0.59, and expressed population signals (EPS) vary between 0.74 and 0.97. The first principal component (PC#1) explains more than 29% of the total variance in all individual series. As a consequence of different sample depth and R_{bt}, the signal-to-noise ratio (SNR) ranges from 2.7 (HB_A) to 36.1 (HP_P) (Table 2). The amount of variance explained by PC#1 and the high SNR values indicate that the chronologies contain strong common signals. The combination of relatively high values of R_{bt} and EPS confirms that our chronologies are suitable for growth–climate relationship studies (Wigley et al., 1984).

Table 3
Correlation coefficients between the eight residual chronologies for the well replicated period 1850–1999.

	BM_A	HB_A	YL_A	BT_P	HP_P	YB_P	YL_P
DX_A	0.53**	0.07	0.22**	0.18*	−0.02	0.10	0.11
BM_A		0.21*	0.18*	0.23**	0.22**	0.22**	0.23**
HB_A			0.38**	0.34**	0.28**	0.26**	0.38**
YL_A				0.10	0.09	0.06	0.47**
BT_P					0.40**	0.34**	0.26**
HP_P						0.42**	0.13
YB_P							0.27**

* Significant at $P < 0.05$.
** Significant at $P < 0.01$.

3.2. Comparison of chronologies

Correlations between chronologies reflect differences caused by species and distance among sites (Table 3). The four fir chronologies display significant inter-site correlations except between DX_A and HB_A, with the highest correlation found between the two highest sites DX_A and BM_A ($R = 0.53$, $P < 0.01$). The four spruce chronologies are correlated significantly among each other except for HP_P and YL_P. Correlation coefficients are higher between neighboring sites of different species (e.g. between YL_A and YL_P) than between distant sites of the same species.

PCA revealed that the first three rotated PCs have eigen values >1 and account for 34%, 17% and 15% of the total variance, respectively, or cumulatively 66% of the total variance (Fig. 3). According to the loadings of the first three PCs, the site chronologies can be divided into three groups. This is consistent with the results of the correlation analyses (Table 3 and Fig. 3). The loadings of PC#1 describe the environmental signals that are common between the *P. brachytyla* chronologies (BT_P, HP_P and YB_P). PC#2 represents the common variances of the two

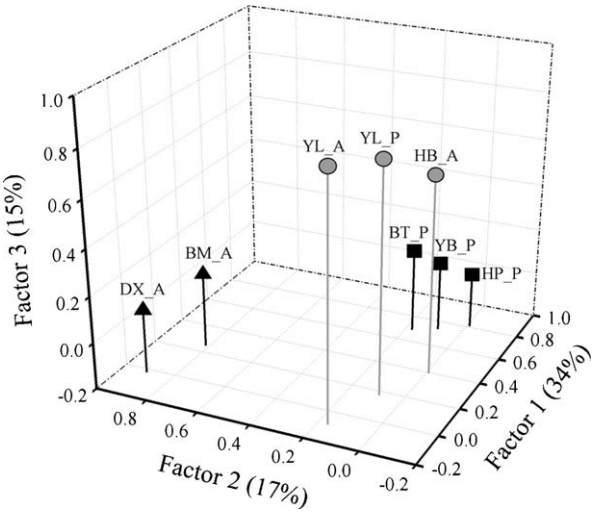

Fig. 3. Relative positions of the eight ring-width chronologies according to the loadings of three significant PCs resulting from principal component analysis over the period 1850–1999. The explained variances of the PCs are indicated in parentheses. The site codes are consistent with those given in Table 1. Groups of similar chronologies are indicated by identical symbols.

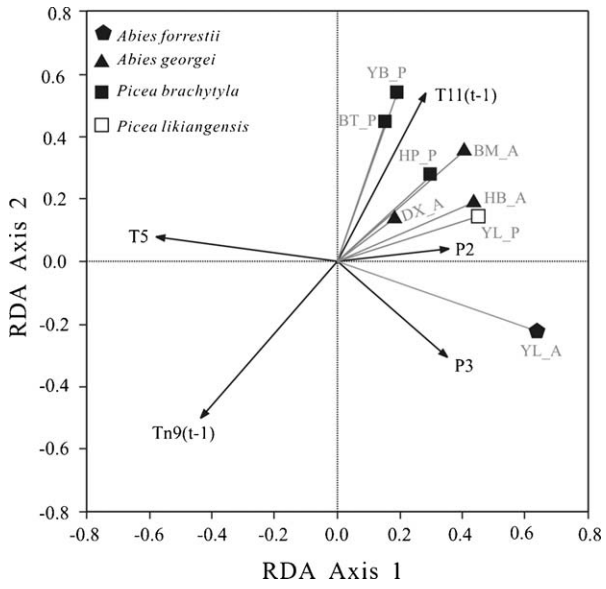

Fig. 4. Redundancy analyses (RDAs) calculated from the eight residual chronologies and the monthly climate parameters for the period 1951–2002. Significant ($P < 0.05$) climate factors are indicated by vectors (black arrows); the longer the vector the more important the climate parameter. The correlation between the variables is illustrated by the cosine of the angle between two vectors. Vectors pointing in nearly the same direction indicate a high positive correlation, vectors pointing in opposite directions have a high negative correlation, and vectors crossing at right angles are related to a near zero correlation (Legendre and Legendre, 1998). P = precipitation, *T* = temperature, Tn = minimum temperature, (t-1) = year before ring formation, and numbers represent months (e.g. 3 = March).

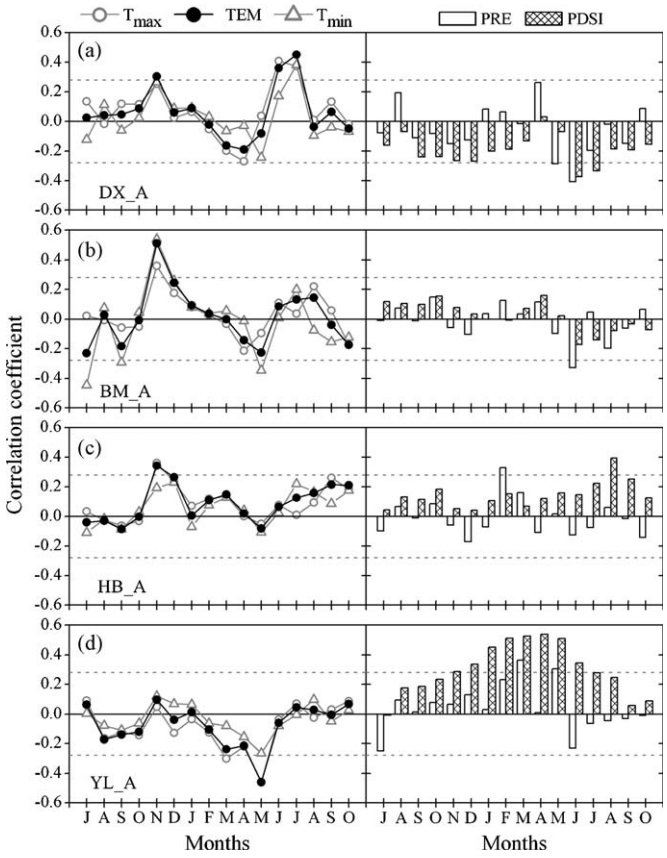

Fig. 5. Correlation between the four fir ring-width residual chronologies and regional monthly maximum (T_{max}), mean (TEM), minimum temperatures (T_{min}), precipitation (PRE) and Palmer drought severity index (PDSI). The correlation coefficients were calculated from previous year July to current year October over the common period 1951–2002. The horizontal dashed lines denote the 95% significance level.

high-elevation sites (DX_A and BM_A) of *A. georgei*. PC#3 encompasses variables of the chronologies at low-elevation sites (YL_A, YL_P and parts of HB_A).

3.3. General climate–growth response

The redundancy analysis (RDA) revealed that November temperature during the year prior to ring formation (T11(t-1)) is the most relevant climatic factor limiting the radial growth of spruce and fir at high- and middle-elevation sites (Fig. 4). Correlation analyses indicated that fir chronologies at high elevations (DX_A and BM_A) are positively correlated with temperatures in the early winter (November–December) prior to growth and in the summer of the growing season (June–August, Table 4 and Fig. 5a and b). Radial growth of spruce trees at middle elevations (BT_P, HP_P and YB_P) is influenced by temperature variations, especially daily maximum temperatures, during winter and early spring season (Table 4 and Fig. 6a–c). The first PC which represents growth variability at middle elevations correlated significantly with winter temperatures ($R = 0.56$ and Fig. 7a) during the period of 1951–1999.

Bräuning (2001) demonstrated that trees in cold-moist environments near the upper treeline in eastern Tibet are sensitive to temperature variations, especially in the winter season. In the west Sichuan Plateau, northeast of our study area, winter minimum temperatures (last December to current February) were found to be the most crucial factor limiting radial growth of Balfour spruce (*Picea balfouriana*) (Shao and Fan, 1999) and some other coniferous species (Wu et al., 2006). Winter temperatures are also found to limit radial growth of *P. crassifolia* in northeastern Tibet (Liang et al., 2006), *Juniperus przewalskii* in the Qilian Mountains (Gou et al., 2007b) and *Picea schrenkiana* in the Tianshan Mountains (Yuan and Li, 1999). Thus, at high-elevation sites, positive growth responses to winter temperatures seem to be a widespread phenomenon in the mountainous area of eastern Tibet.

Table 4
Correlation coefficients between eight residual chronologies and seasonal climatic variables of monthly mean temperature (TEM), precipitation (PRE) and Palmer drought severity index (PDSI) for the period 1951–2002 ($n = 53$).

Climatic variable	DX_A	BM_A	HB_A	YL_A	BT_P	HP_P	YB_P	YL_P
TEM (p8-p9)	0.06	−0.13	−0.07	−0.21	−0.38**	−0.11	−0.31*	−0.23
TEM (p11-p12)	0.22	0.42**	0.30*	0.00	0.23	0.36**	0.46**	0.06
TEM (p11-2)	0.12	0.26	0.21	−0.05	0.31*	0.47**	0.49**	−0.005
TEM (6–8)	0.48**	0.20	0.19	−0.01	0.00	0.07	0.08	0.06
PRE (3–5)	−0.13	−0.02	0.03	0.42**	−0.23	0.08	−0.22	0.10
PDSI (3–5)	0.09	−0.07	0.13	0.59**	−0.04	0.30*	0.06	0.30*

The numbers in the parentheses represent consecutive number of months, while p indicates the year before ring formation.
* Significant at $P < 0.05$.
** Significant at $P < 0.01$.

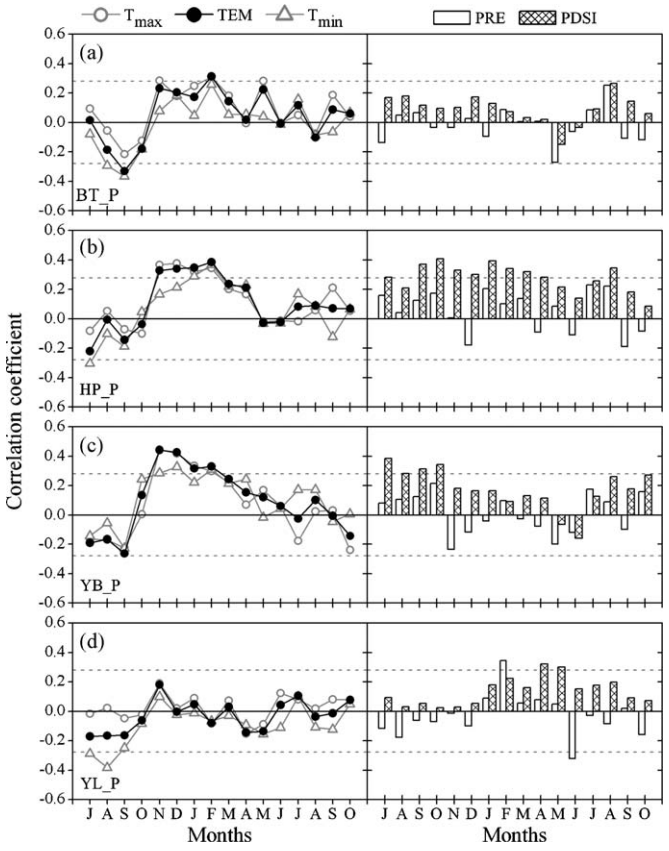

Fig. 6. Correlation between four spruce ring-width residual chronologies and regional monthly maximum (T_{max}), mean (TEM), minimum temperatures (T_{min}), precipitation (PRE) and Palmer drought severity index (PDSI). The correlation coefficients were calculated from previous year July to current year October over the common period 1951–2002. The horizontal dashed lines indicate the 95% significance level.

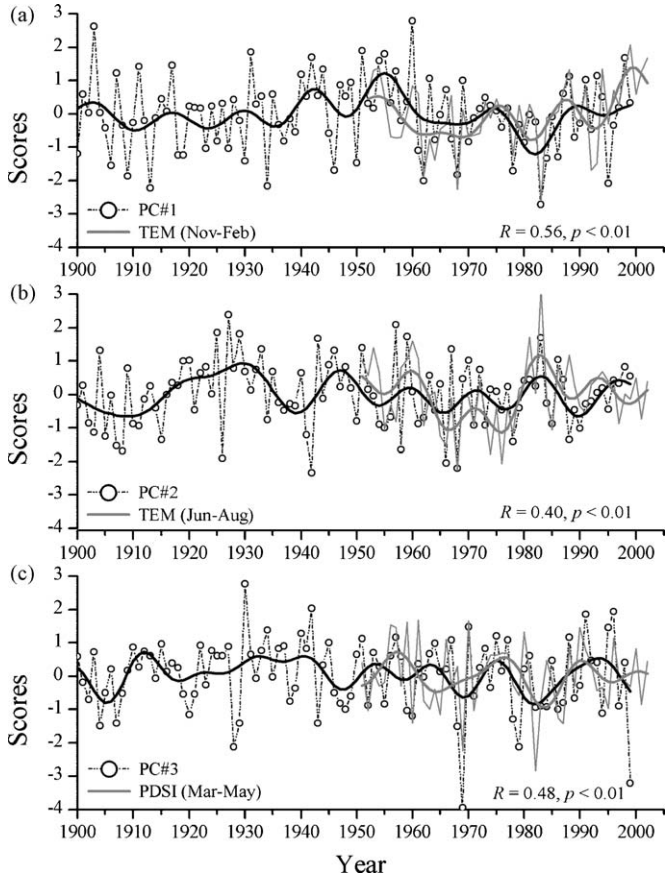

Fig. 7. Comparisons of (a) PC#1 with winter (prior November–February) mean temperature, (b) PC#2 with summer (June–August) mean temperature and (c) PC#3 with spring (March–May) PDSI. Values are adjusted for their mean and standard deviations. Bolded lines are smoothed with a 10-year low-pass filter. *R* indicates the linear correlation coefficients between PCs and climatic variables over the period 1951–1999 and *P* denotes their significant levels.

However, similar reaction patterns are also documented for other humid mountain regions of the world. Winter temperature has also been found to influence radial growth of various tree species in northeastern America (Pederson et al., 2004). In the north Cascade Mountains, Peterson and Peterson (1994) found that growth of four species correlated positively with previous November temperatures, but negatively with early spring precipitation and snow-pack depths. After cold winters with delayed snow melt, the following vegetation period is shortened, which may lead to a reduced early wood width in the following year (Ettl and Peterson, 1995; Peterson and Peterson, 2001; Vaganov et al., 1999).

The detrimental effect of low winter temperatures on tree growth, especially at treeline sites, supports the hypothesis that winter temperature is one of the dominant controls on the location of the timberline ecotone (Körner, 1998). Vegetation buds, which are active until mid-October or later, are not fully cold harden until the coldest month (January) and can be damaged by cold nighttime temperature (Hawkins, 1993; Taschler and Neuner, 2004). As recorded from the Shangri-la station, T_{max} and T_{min} in November range from 8.5 to 13.7 °C and from −15.4 to −2.8 °C, respectively. Daily temperature range (DTR) in November ranges from 12.1 to 22 °C. A maximum difference of about 15.1 °C between T_{max} and T_{min} in November may cause direct frost damage to needles and buds and may reduce root activity or increase the risk of frost desiccation (Jalkanen et al., 1998; Körner, 1998; Neuner, 2007), since solar radiation in the Hengduan Mountains is considerable high during winter times. Defoliation and bud mortality deplete the pool of stored carbohydrates and reduce a tree's potential for future growth and photosynthetic capture, thus reduce radial growth during the following year (Lazarus et al., 2004; Misson et al., 2004). Winter carbon shortage, as demonstrated by insufficient non-structural carbohydrates (NSC) and the sugar-to-starch ratio, has been suggested to influence the survival and growth of coniferous trees at the upper treeline on the eastern edge of the Tibetan Plateau (M. Li et al., 2008). Moreover, in mild late winters, trees are particularly likely to suffer from enhanced desiccation as a result of increased transpiration rates of needles and shoots, photoinhibitory stress and short-term fluctuations in shoot temperatures, leading to xylem embolism (Sperry et al., 1994; Pederson et al., 2004).

3.4. Site-specific climate–growth responses

The effects of steep environmental gradients on forest composition and patterns of stand development in the central Hengduan Mountains are well documented (i.e. Yang and Shen, 1984; Yu et al., 1989). The results of this study emphasize that these gradients cause markedly diverse patterns of tree-growth responses to climatic variations. Conifers growing at high and middle elevations are mainly limited by temperature variations, whereas moisture availability in the spring season is more important at lower elevation sites (Table 4 and Figs. 5 and 6). At middle-elevation site of HB_A, fir growth is less sensitive to climate variability (Fig. 5c). At inter-annual to decadal scales, there are generally agreements between PC#2 and summer temperatures

($R = 0.40$; Fig. 7b), as well as between PC#3 and spring PDSI ($R = 0.48$; Fig. 7c).

At low-elevation sites (i.e. YL_A and YL_P), spring precipitation is the most important factor for growth, and temperature in May (T5) is negatively associated with radial growth (Figs. 4, 5d and 6d). This is also clearly reflected by the reaction to PDSI. High-elevation fir sites (DX_A and BM_A) show negative correlations, whereas the low-elevation fir site (YL_A) shows positive correlations with PDSI (Fig. 5). For spruce, this picture looks different, since absolute elevations of spruce sites are lower than for fir (Table 1). Nevertheless, the highest spruce site (BT_P) shows lower correlations to PDSI than all other sites. These findings confirm that water supply during the spring season is crucial for tree growth at low elevations. On the other hand, the climate diagram of Lijiang station that is close to the two low-elevation sites showed a relative dry period during the pre-monsoon season (Fig. 2). Tree growth benefit from enhanced soil moisture content during the early part of the growing season, while after the onset of the summer monsoon season, enough moisture is available to satisfy the water demand of the trees (Bräuning and Grießinger, 2006).

Precipitation in June has a negative influence on radial growth at higher elevations, especially at the upper treeline sites DX_A and BM_A. At high-elevation sites, abundant rainfall is generally combined with enhanced cloudiness and reduced radiation input and lower temperatures. Monthly mean temperatures (TEM) and monthly precipitation (PRE) in May and June show inverse correlations of -0.56 and -0.54 ($P < 0.01$), respectively. As a consequence of abundant rainfall during early summer (May–June), tree growth at high elevations is constrained by light availability and temperature (e.g. Graham et al., 2003; Bräuning and Mantwill, 2004).

3.5. Species-specific climate–growth responses

Fir and spruce trees show a different climate-response behavior, both seasonally and in magnitude (Figs. 5 and 6). Compared with spruce, fir responds to winter temperature variations within a narrower seasonal window, mostly confined to November of the year prior to growth. In the summer season (June–August), low temperatures limit radial growth of fir more severely than growth of spruce (compare Figs. 5 and 6). Hence, tree-ring chronologies from high-elevation conifer sites might be used to reconstruct winter monsoon intensity. For spruce at middle elevations, warm conditions in the growing season have a positive effect on radial growth, but most of the correlations found are not statistically significant (Table 4 and Fig. 6).

Radial growth of spruce trees correlates negatively with temperatures in the late summer of the previous year, which is accompanied by a positive influence of precipitation in the same season (Fig. 6). Lagged effects of summer temperature and precipitation on growth in the following year are commonly observed in tree-ring studies of subalpine conifers (Villalba et al., 1994; Ettl and Peterson, 1995; Tardif and Stevenson, 2001). Warm and dry late summers can reduce the accumulation of carbohydrate reserves by limiting photosynthesis through drought stress, by increasing respiration rate, and by diverting energy reserves to current year growth (Fritts, 1976; Rolland and Schueller, 1994). At low-elevation sites, growth of *A. forrestii* is more severely restricted by spring moisture availability than growth of *P. likiangensis*, indicating that this spruce species is more tolerant of droughts (compare Figs. 5d and 6d).

4. Conclusions

We compared tree-ring width chronology characteristics and climate–growth responses of high-elevation conifers along an elevation gradient in the central Hengduan Mountains. As indicated by correlation analyses and PCA, tree-ring chronologies from different altitudinal belts can be distinguished by their climate–growth relationships. In general, the climate–growth relationships found at different altitudes in this region resemble the reaction patterns found in other humid mountain systems on the Tibetan Plateau. Winter temperatures are found to be the most consistent climatic factor limiting radial growth of fir and spruce at high to middle elevations. However, the magnitude and seasonal domain of growth responses to climate are species- and habitat-specific. At lower elevations, tree growth is limited by spring moisture availability. In the study area, regional temperatures have been increasing significantly since the 1960s, by 0.04 °C year^{-1} and 0.022 °C year^{-1} for winter (prior November–February) and summer season (June–August), respectively (Fig. 7a and b). During the past two decades, enhanced tree growth anomalies at high- to middle-elevation sites are evident. Under the current warming trend, high- to middle-elevation conifers may benefit from increasing temperatures, especially from rising winter temperatures in the central Hengduan Mountains. Incorporation of species-specific climate–growth reactions into simulation models may be helpful to clarify the biogeographic problems of the Pleistocene refuge areas of Chinese conifers (Frenzel et al., 2003) and to refine forecast models of the regional impact of climate change on the forests in the central Hengduan Mountains.

Acknowledgements

The authors thank Mrs. Iris Burchardt for her aid on tree-ring measurements. We thank Di Cheng-Qiang for field assistance. Particular thanks are extended to anonymous reviewers for their valuable suggestions and comments regarding revision of the manuscript. This work was financially supported by the National Science Foundation of China (grant No. 30670320) and the Max-Planck-Gesellschaft.

References

Anfodillo, T., Rento, S., Carraro, V., Furlanetto, L., Urbinati, C., Carrer, M., 1998. Tree water relations and climatic variations at the alpine timberline: seasonal changes of sap flux and xylem water potential in *Larix decidua* Miller, *Picea abies* (L.) Karst. and *Pinus cembra* L. Annals of Forest Science 155, 159–172.

Blasing, T.J., Solomon, A.M., Duvick, D.N., 1984. Response functions revisited. Tree-Ring Bulletin 44, 1–15.

Böhner, J., 2006. General climatic controls and topoclimatic variations in Central and High Asia. Boreas 35, 279–295.

Bräuning, A., 1994. Dendrochronology for the last 1400 years in eastern Tibet. GeoJournal 34, 75–95.

Bräuning, A., 2001. Combined view of various tree ring parameters from different habitats in Tibet for the reconstruction of seasonal aspects of Asian Monsoon variability. The Palaeobotanist 50, 1–12.

Bräuning, A., Mantwill, B., 2004. Summer temperature and summer monsoon history on the Tibetan Plateau during the last 400 years recorded by tree rings. Geophysical Research Letters 31 , doi:10.1029/2004GL020793 L24205.

Bräuning, A., Grießinger, J., 2006. Late Holocene variations in monsoon intensity in the Tibetan-Himalayan region—evidence from tree rings. Journal of the Geological Society of India 69 (3), 485–494.

Briffa, K.R., Schweingruber, F.H., Jones, P.D., Osborn, T.J., Shiyatov, S.G., Vaganov, E.A., 1998. Reduced sensitivity of recent tree-growth to temperature at high northern latitudes. Nature 391, 678–682.

Carrer, M., Anfodillo, T., Urbinati, C., Carraro, V., 1998. High-altitude forest sensitivity to global warming: results from long-term and short-term analyses in the Eastern Italian alps. In: Beniston, M., Innes, J.L. (Eds.), The Impacts of Climate Variability of Forest. Springer-Verlag, Berlin, Heidelberg, pp. 171–189.

Cook, E.R., 1985. A time-series analysis approach to tree-ring standardization. Ph.D. Dissertation. The University of Arizona Press, Tucson.

Cook, E.R., Kairiukstis, A., 1990. Methods of Dendrochronology: Applications in the Environmental Sciences. Kluwer Academic Press, Dordrecht.

Cook, E.R., Peters, K., 1997. Calculating unbiased tree-ring indices for the study of climatic and environmental change. The Holocene 7, 361–370.

Dai, A., Trenberth, K.E., Qian, T., 2004. A global data set of Palmer Drought Severity Index for 1870–2002: relationship with soil moisture and effects of surface warming. Journal of Hydrometeorology 5, 1117–1130.

Ettl, G.J., Peterson, D.L., 1995. Growth response of subalpine fir (*Abies lasiocarpa*) to climate in the Olympic Mountains, Washington, USA. Global Change Biology 1, 213–230.
Fan, Z., Bräuning, A., Cao, K., 2008. Tree-ring based drought reconstruction in the central Hengduan Mountains region (China) since AD 1655. International Journal of Climatology 28, 1879–1887.
Frenzel, B., Bräuning, A., Adamczyk, S., 2003. On the problem of possible late-glacial forest refuge-area with the deep valleys of Eastern Tibet. Erdkunde 57, 182–198.
Fritts, H.C., 1976. Tree Rings and Climate. Academic Press, London.
Girardin, M.P., Tardif, J.C., Flannigan, M.D., Bergeron, Y., 2006. Synoptic-scale atmospheric circulation and boreal Canada summer drought variability of the past three centuries. Journal of Climate 19, 1922–1947.
Gou, X., Chen, F., Yang, M., Li, J., Peng, J., Jin, L., 2005. Climatic response of thick leaf spruce (*Picea crassifolia*) tree-ring width at different elevations over Qilian Mountains, northwestern China. Journal of Arid Environments 61, 513–524.
Gou, X., Chen, F., Cook, E.R., Jacoby, G.C., Yang, M., Li, J., 2007a. Streamflow variations of the Yellow River over the past 593 years in western China reconstructed from tree rings. Water Resources Research 43 , doi:10.1029/2006WR005705 W06434.
Gou, X., Chen, F., Jacoby, G.C., Cook, E.R., Yang, M., Peng, J., Zhang, Y., 2007b. Rapid tree growth with respect to the last 400 years in response to climate warming, northeastern Tibetan Plateau. International Journal of Climatology 27, 1497–1503.
Graham, E.A., Mulkey, S.S., Kitajima, K., Phillips, N.G., Wright, S.J., 2003. Cloud cover limits net CO_2 uptake and growth of a rainforest tree during tropical rainy seasons. Proceedings of the National Academy of Sciences 100, 572–576.
Hawkins, B.J., 1993. Photoperiod and night frost influence on the frost hardness of *Chamaecyparis nootkatensis*. Canadian Journal of Forest Research 23, 1408–1414.
Jalkanen, R., Aalto, T., Kurkela, T., 1998. Revealing past needle density in *Pinus* spp. Scandinavian Journal of Forest Research 13, 292–296.
Körner, C., 1998. A re-assessment of high elevation treeline positions and their explanation. Oecologia 115, 445–459.
Lazarus, B.E., Schaberg, P.G., DeHayes, D.H., Hawley, G.J., 2004. Severe red spruce winter injury in 2003 creates unusual ecological event in the northeastern United States. Canadian Journal of Forest Research 34, 1784–1788.
Legendre, P., Legendre, L., 1998. Numerical Ecology. Elsevier Scientific, New York.
Li, J., Cook, E.R., D'Arrigo, R., Chen, F., Gou, X., Peng, J., Huang, J., 2008. Common tree growth anomalies over the northeastern Tibetan Plateau during the last six centuries: implications for regional moisture change. Global Change Biology 14, 1–12.
Li, M., Xiao, W., Wang, S., Cheng, G., Cherubini, P., Cai, X., Liu, X., Wang, X., Zhu, W., 2008. Mobile carbohydrates in Himalayan treeling trees I. Evidence for carbon gain limitation but not for growth limitation. Tree Physiology 28, 1287–1296.
Liang, E., Shao, X., Eckstein, D., Huang, L., Liu, X., 2006. Topography- and species-dependent growth responses of *Sabina prezewalskii* and *Picea crassifolia* to climate on the northeast Tibetan Plateau. Forest Ecology and Management 236, 268–277.
Liang, E., Shao, X., Qin, N., 2008. Tree-ring based summer temperature reconstruction for the source region of the Yangtze River on the Tibetan Plateau. Global and Planetary Change 63, 313–320.
Liu, L., Shao, X., Liang, E., 2006. Climate signals from tree ring chronologies of the upper and lower treelines in the Dulan region of the northeastern Qinghai-Tibetan Plateau. Journal of Integrative Plant Biology 48 (3), 278–285.
Misson, L., Rathgeber, C., Guiot, J., 2004. Dendroecological analysis of climatic effects on *Quercus petraea* and *Pinus halepensis* radial growth using the process-based MAIDEN model. Canadian Journal of Forest Research 34, 888–898.
Mitchell, T.D., Jones, P.D., 2005. An improved method of constructing a database of monthly climate observations and associated high resolution grids. International Journal of Climatology 25, 693–712.
Neuner, G., 2007. Frost resistance at the upper timberline. In: Wieser, G., Tausz, M. (Eds.), Trees at their upper limit—treelife limitation at the alpine timberline. Springer, Dordrecht, The Netherlands, pp. 171–180.
Osborn, T.J., Briffa, K.R., Jones, P.D., 1997. Adjusting variance for sample-size in tree-ring chronologies and other regional mean time series. Dendrochronologia 15, 89–99.
Pederson, N., Cook, E.R., Jacoby, G.C., Peteet, D.M., Griffin, K.L., 2004. The influence of winter temperatures on the annual radial growth of six northern range margin species. Dendrochronologia 22, 7–29.
Peng, J., Gou, X., Chen, F., Li, J., Liu, P., Zhang, Y., 2008. Altitudinal variability of climate–tree growth relationships along a consistent slope of Anyemaqen Mountains, northeastern Tibetan Plateau. Dendrochronologia 26 (2), 87–96.
Peterson, D.W., Peterson, D.L., 1994. Effects of climate on radial growth of subalpine conifers in the North Cascade Mountains. Canadian Journal of Forest Research 24, 1921–1932.
Peterson, D.W., Peterson, D.L., 2001. Mountain hemlock growth responds to climatic variability at annual and decadal time scales. Ecology 82, 3330–3345.
Rinn, F., 2003. TSAP-Win: Time Series Analysis and Presentation for Dendrochronology and Related Applications. Version 0.55 User reference. Heidelberg, Germany (http://www.rimatech.com).
Rolland, C., Schueller, J., 1994. Relationships between mountain pine and climate in the French Pyreness (Font-Romeu) studies using the radiodensitometrical method. Pirineos 43–144, 55–70.
Saxe, H., Cannell, M.G.R., Johnsen, B., Ryan, M.G., Vourlitis, G., 2001. Tree and forest functioning in response to global warming. New Phytologist 149, 369–399.
Schweingruber, F.H., 1996. Tree Rings and Environment-Dendrochronology. Haupt, Bern, p. 609.
Shao, X., Fan, J., 1999. Past climate on west Sichuan plateau as reconstructed from ring-widths of dragon spruce. Quaternary Science 1, 81–89 (in Chinese, with English abstract).
Shao, X., Huang, L., Liu, H., Liang, E., Fang, X., Wang, L., 2005. Reconstruction of precipitation variation from tree rings in recent 1000 years in Delingha, Qinghai. Science in China (Series D) 48, 939–949.
Sheppard, P.R., Tarasov, P.E., Graumlich, L.J., Heussner, K.U., Wagner, M., Österle, H., Thompson, L.G., 2004. Annual precipitation since 515 BC reconstructed living and fossil juniper growth of northeastern Qinghai Province, China. Climate Dynamics 23, 869–881.
Sperry, J.S., Nichols, K.L., Sullivan, J.E.M., Eastlack, S.E., 1994. Xylem embolism in ring-porous, diffuse-porous, and coniferous trees of northern Utah and interior Alaska. Ecology 75, 1736–1752.
Stokes, M.A., Smiley, T.L., 1968. An Introduction to Tree-Ring Dating. The University of Chicago Press, Chicago, London, p. 73.
Tardif, J.C., Stevenson, D., 2001. Radial growth–climate association of *Thuja occidentalis* L. at the northwestern limit of its distribution, Manitoba, Canada. Dendrochronologia 19 (2), 179–187.
Tardif, J.C., Conciatori, F., Nantel, P., Gagnon, D., 2006. Radial growth and climate responses of white oak (*Quercus alba*) and northern red oak (*Quercus rubra*) at the northern distribution limit of white oak in Quebec, Canada. Journal of Biogeography 33, 1657–1669.
Taschler, D., Neuner, G., 2004. Summer frost resistance and freezing patterns measured *in situ* in leaves of major alpine plant growth forms in relation to their upper distribution boundary. Plant, Cell and Environment 24, 737–746.
ter Braak, C.J.F., Smilauer, P., 2002. CANOCO Reference Manual and CanoDraw for User's Guide Windows: Software for Canonical Community Ordination, Version 4.5. Microcomputer Power, Ithaca, NY.
Tessier, L., Guibal, F., Schweingruber, F.H., 1997. Research strategies in dendroecology and dendroclimatology in mountain environments. Climatic Change 36, 499–517.
The Editing Committee of "The Baima National Nature Reserve", 2003. The Baima National Nature Reserve. Yunnan Nationality Press, Kunming, pp. 31–50 (in Chinese).
Thuiller, W., Lavorel, S., Arujo, M.B., Sykes, M.T., Prentice, I.C., 2005. Climate change threats to plant diversity in Europe. Proceedings of the National Academy of Sciences 102, 8245–8250.
Tian, Q., Gou, X., Zhang, Y., Peng, J., Wang, S., Chen, T., 2007. Tree-ring based drought reconstruction (A.D. 1855–2001) for the Qilian Mountains, Northwestern China. Tree-Ring Research 63 (1), 27–36.
Trouet, V., Haneca, K., Coppin, P., Beeckman, H., 2001. Tree ring analysis of *Brachystegia spiciformis* and *Isoberlinia tomentosa*: evaluation of the ENSO-signal in the Miombo woodland of eastern Africa. IAWA Journal 22, 385–399.
Vaganov, E.A., Hughes, M.K., Kirdyanov, A.V., Schweingruber, F.H., Silkin, P.P., 1999. Influence of snowfall and melt timing on tree growth in subarctic Eurasia. Nature 400, 149–151.
Villalba, R., Veblen, T.T., Ogden, J., 1994. Climatic influences on the growth of subalpine trees in the Colorada Front Range. Ecology 75, 1450–1462.
Wigley, T., Briffa, K.R., Jones, P.D., 1984. On the average value of correlated time series, with applications in dendroclimatology and hydrometeorology. Journal of Applied Meteorology 23, 201–213.
Wu, P., Wang, L., Huang, L., 2006. A preliminary study on the tree-ring sensitivity to climate change of five endemic conifer species in China. Geographical Research 25 (1), 43–52 (in Chinese, with English abstract).
Wu, X., Lin, Z., Sun, L., 1988. A preliminary study of the climatic change of the Hengduan Mountains area since 1600 A.D. Advances in Atmospheric Science 5, 437–443.
Yang, Q.Y., Shen, K.D., 1984. On vertical zonation of the Northwestern Yunnan. Acta Geographica Sinica 39 (2), 141–147 (in Chinese, with English abstract).
Yu, Y., Liu, L., Zhang, J., 1989. Vegetation regionalization of the Hengduan Mountains region. Mountain Research 7 (1), 47–55 (in Chinese, with English abstract).
Yuan, Y., Li, J., 1999. Reconstruction and analysis of 450 years winter temperature series in Urumqi River Source of Tianshan Mountains. Journal of Glaciology and Geocryology 21 (1), 64–70 (in Chinese, with English abstract).
Zhang, Q., Cheng, G., Yao, T., Kang, X., Huang, J., 2003. A 2,326-year tree-ring records of climate variability on the northeastern Qinghai-Tibetan Plateau. Geophysical Research Letters 30 , doi:10.1029/2003GL017425 L141739.
Zhang, Y.G., 1998. Several issues concerning vertical climate of the Hengduan Mountains. Resources Science 20, 12–19 (in Chinese).
Zheng, D., 1996. The system of physico-geographical region of the Qinghai-Xizang (Tibet) Plateau. Science in China (Series D) 39, 410–417 (in Chinese, with English abstract).